Analytica Chimica Acta 1125 (2020) 50–56

Contents lists available at ScienceDirect

Analytica Chimica Acta

journal homepage: www.elsevier.com/locate/aca

Fully automatic integrated continuous-flow digital PCR device for absolute DNA quantification

Yangyang Jiang [a], Andreas Manz [c, d], Wenming Wu [a, b, *]

[a] State Key Laboratory of Applied Optics, Changchun Institute of Optics, Fine Mechanics and Physics, Chinese Academy of Sciences, Changchun, 130033, China
[b] University of Chinese Academy of Sciences, Beijing, 100049, China
[c] Systems Engineering Department, Saarland University, 66123, Saarbrücken, Germany
[d] Bio Sensor & Materials Group, KIST Europe, 66123, Saarbrücken, Germany

HIGHLIGHTS

The highlights of the manuscript as follow:•Single device for digital PCR detection.
•Solar cells drive, no external power supply.
•A software was designed which can control the system and analyze the data.
•Absolute quantitative detection of hepatitis B virus in human serum.

GRAPHICAL ABSTRACT

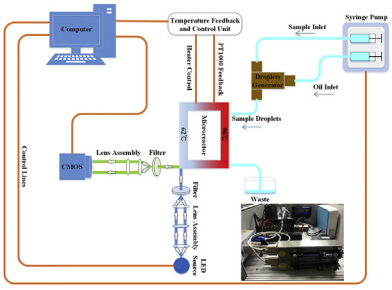

ARTICLE INFO

Article history:
Received 2 February 2020
Received in revised form
27 April 2020
Accepted 2 May 2020
Available online 23 May 2020

Keywords:
Microfluidics
Digital PCR
Fully automatic
Contiuous flow
Integrated device

ABSTRACT

Existing digital polymerase chain reaction (PCR) devices consist of multiple independent devices, such as a droplet generator, a PCR thermocycler, and a droplet reader, which have the disadvantages of low integration, complex equipment structure, and high operation difficulty. This paper proposes a fully automatic integrated digital PCR device based on continuous-flow digital PCR theory. By simply adding the sample to the entrance of the integrated instrument, a series of procedures required for digital PCR detection can be fully automated, including sample injection, droplet generation, PCR thermal cycling, fluorescence acquisition, and signal analysis. In contrast to traditional techniques, sample testing requires only one integrated device rather than three separate instruments. For full automation, we design complete control and data processing software, which can complete a test by one-step operation. Therefore, the disadvantages of traditional instruments, such as multi-step operation, and hence, potential environmental pollution, are avoided. Moreover, the system can be powered by solar cells and does not require an external power supply.

As a proof of concept, the proposed device is used for absolute quantitative detection of the hepatitis B virus in serum samples. The capacity of the system is validated by absolute quantification of three orders of magnitude from 10^3 to 10^5 IU/mL. The results have a good linear correlation (0.9986) with those of the traditional quantitative (qPCR), thus confirming the reliability of the instrument. In summary, we believe that our work can promote the development of integrated digital PCR systems.

* Corresponding author. State Key Laboratory of Applied Optics, Changchun Institute of Optics, Fine Mechanics and Physics, Chinese Academy of Sciences, Changchun, 130033, China.
E-mail address: wuwm@ciomp.ac.cn (W. Wu).

https://doi.org/10.1016/j.aca.2020.05.044
0003-2670/

1. Introduction

Previously, we reported the first "micro total analysis system" (μTAS, also known as a microfluidic or lab-on-a-chip system) in the world [1], which has shown considerable potential in chemistry [2,3] and biotechnology [4–6], owing to its advantage of high efficiency, low cost, and portability. Microdroplet technology is an important part of microfluidics; it is widely used in biochemistry analyses, such as single-cell sequencing [7,8], drug delivery, cell screening, microreactor studies [9,10], and nucleic acid analysis [11]. As one of the important frontier application fields of microfluidics, the digital droplet polymerase chain reaction (ddPCR) uses microdroplet technology. It is an advanced tool that allows the quantification of nucleic acid without the need for any standard reference [12,13]. Digital PCR has the advantages of high detection sensitivity, high quantitative precision, and high tolerance. It is used in copy number variation [14–16], mutation detection, relative gene expression research (such as allele imbalance expression), next-generation sequencing result verification, microRNA expression analysis, single-cell gene expression analysis, etc.

At present, most representative commercial digital PCR instruments consist of multiple independent sub-devices. The realization process can be divided into three parts:

(1) Sample distribution: The oil phase and the sample (water phase) are placed on the droplet generation chip, and sealed and placed in the droplet generator. The water phase is dispersed into thousands of microdroplets [17–19] and submerged in fluorinated oil. Another method of sample partitioning is used by microwell chips [20–22], whereby the sample is loaded into many reaction wells and each reaction well is isolated from its neighbors.
(2) PCR amplification: The generated droplets are transferred to the EP tube and inserted into the pore plate of the PCR instrument or placed on the microwell chip on the in-situ plate of the PCR instrument. The PCR reagent undergoes a series of thermal cycles to generate millions of DNA copies in the reaction chambers containing templates.
(3) Optical detection: The flowing droplets are detected by widely used sensors such as phototransistor, photodiode, or photomultiplier tubes [23,24]. The static chip usually implements detection via scanning devices such as complementary metal-oxide-semiconductor (CMOS) sensors or charge-coupled devices (CCDs) [25–27]. The optical devices can capture fluorescence light emitted by fluorophores in the TaqMan probe or fluorescence dye and measure the light intensity.

Thus, current methods require multi-step operation to transfer samples between a series of devices, which may cause contamination during the reaction process. In addition, manual operations between several functional units depend on specially trained operators and may hence not meet the requirements of widespread use by non-professional technical personnel. Moreover, the design of multiple operating units increases the cost of equipment and consumables of the entire system. For example, the droplet generator requires expensive chip consumables. The microwell digital PCR system requires a professional chip loader to load and seal the chips. The Droplet Digital PCR System not only relies on expensive droplet generation chips and oils but also requires a bulky pneumatic pump and interfaces that connect the specific hip to a pressure source, which provides power for droplet generation [28,29] and generates water-in-oil droplets through the droplet generation chip. Droplet reaction is realized by a temperature cycler with the disadvantages of large volume, high energy consumption, and high cost. Owing to the above-mentioned shortcomings, it is extremely difficult to use a set of digital PCR instruments in the POCT field. Moreover, ordinary laboratories cannot afford such expensive instruments. Current commercially available systems require an external power supply and they can only be used in professional laboratories with complete power systems. Thus, they cannot be effectively employed in many fields that require rapid on-site diagnosis, such as disease prevention and control, crop screening, and biochemical warfare agent detection.

The above-mentioned issues highlight the need for a portable, integrated, and low-cost ddPCR device that does not require an external power supply [30–33]. Furthermore, such a device should be energy-efficient and easy to handle for users.

Here, we present the all-in-one digital PCR instrument to realize automatic integration for the first time in the world. The entire detection process, including the workflow (fluid control, temperature control, fluorescence collection, and data analysis), is controlled by a notebook. The overall volume of the device is only 467 × 420 × 185 mm (width x depth x height). Furthermore, the device features an in-built energy source (solar cells), and it has strong environmental adaptability and high portability. In addition, a self-designed fluorescence analysis system is embedded in the instrument. The optical detection is a three-step process. The first step is fluorescent excitation of the PCR microreactor with specific wavelengths of light. Then, the fluorescence droplets are captured in the microfluidic channel using a CMOS camera. Finally, data processing of the captured images and subsequent quantification are performed.

We believe that the proposed device has considerable potential for on-site detection in various remote environments without the intervention of professional laboratories.

2. Methods

2.1. Assembly of microdroplet-based continuous-flow digital PCR device

The digital PCR device consists of five subsystems: sample transporter and microdroplet generator, microreactor, fluorescence imaging system, reagent refrigerator, and center controller and power management system. The subsystems and workflow flow are shown in Fig. 1.

The sample transporter and microdroplet generator consists of two 1-mL syringes, two syringe pumps, two fine needles, and a Teflon tube (i.d. = 0.15 mm, o.d. = 0.4 mm). The oil phase (7500, Huizhen, Suzhou, China) was added to the two syringes, which were then connected to the Teflon tube by two 34-gauge needles. The oil phase was filled in the Teflon tube and further connected with a waste bottle at the end of outlet. The syringes were installed in syringe pumps that provided power for transporting the sample and generating droplets.

CNC-processed copper plates were placed over the ceramic heaters (width = height = 40 mm, 5 V, 8 W), which were embedded with PT1000 thermistors (Hayashi Denko, Japan). The heater was placed in parallel with another heater, and they were separated by isolation columns. Then, the Teflon tube was wrapped around the heating unit for around 40 cycles. The two heaters were used to maintain the denaturation (96 °C) and annealing/extension (62 °C) temperatures, respectively. They were regulated by a PID temperature controller with an accuracy of ±0.1 °C based on the sensor feedback. This device is the core unit of the microreactor.

The fluorescence imaging system consists of an LED (XPE3W, Cree, NC) with a dominant wavelength of 470 nm and a condensing lens, a CMOS camera (E3ISPM20000KPA, Kuy Nice, China) with a magnifying lens (Chuang Wei, China), and two commercial filters (Xintian Bori, Beijing, China). The excitation light from the LED,

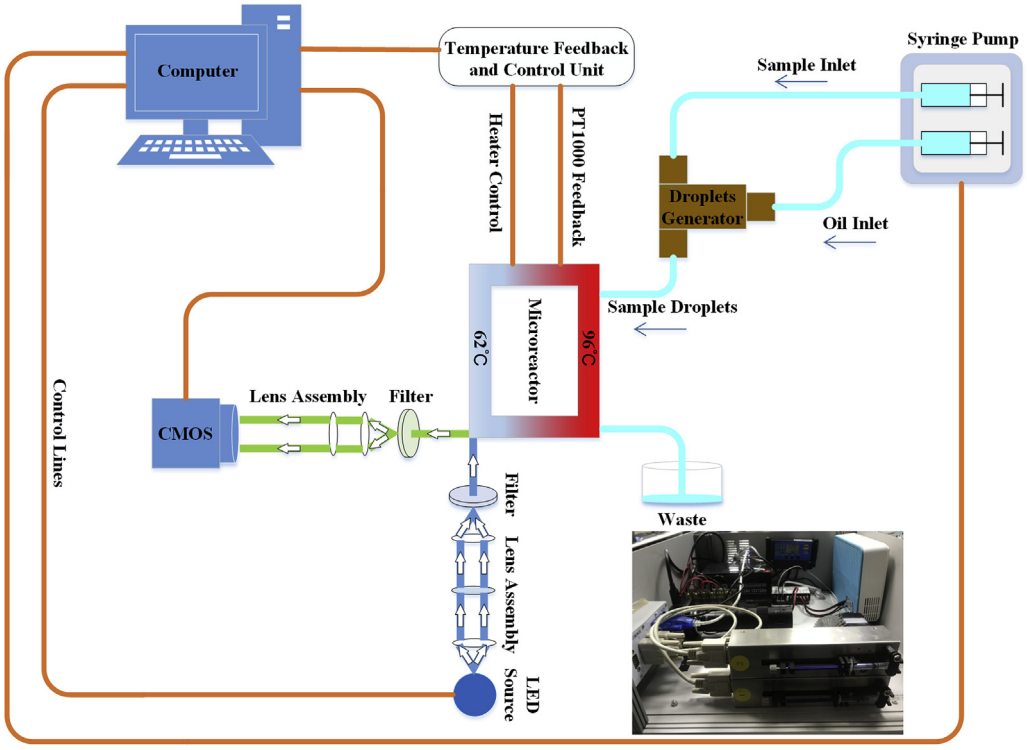

Fig. 1. Schematic illustration of the system architecture of the continuous-flow digital PCR instrument. Sample injection takes place through the droplet generator, and the sample is then fed through the microreactor while the fluorescence intensity is measured by the optical module.

which was filtered by a band-pass excitation filter (470 ± 20 nm), was used to excite the FAM probe. The 500 nm cut-off emission filter was fixed in front of the CMOS lens, which captured the fluorescence droplet images. The images could be transmitted to our laptop by a USB cable.

2.2. Reagent refrigerator

The digital PCR device has a built-in refrigeration box (Dometic, Shenzhen, China) for preserving the PCR reagents. The refrigerator can maintain the reagents at 4 °C to prolong their storage life. To confirm that the device can be used as a digital PCR device, a commercial real-time qPCR device (Connect, Bio Rad, CA) was considered as a reference. The hepatitis B virus DNA quantitative diagnostic kit (NEPG Liaoning Bio-Pharma Co., Ltd., China) consists of nucleic acid extraction reagents (HBV lysis buffer, magnetic bead suspensions, HBV rinse buffer, HBV eluent buffer), nucleic acid amplification reagents (HBV PCR reaction mixture, HBV enzyme mixture), and HBV reference standard solutions (1×10^3–1×10^5 IU/mL). The reference standard serum solutions were extracted using the nucleic acid extraction reagents. Each PCR reagent consisted of 18 μL of the reaction mixture (i.e., solution containing primers, probes, dNTP, etc.), 2 μL of the DNA polymerase mixture (i.e., enzyme preparation containing Taq, UDG enzymes, etc.), and 30 μL of nucleic acid solution.

2.3. Preparing and loading the sample

First, the template DNA was extracted by magnetic bead extraction in five steps. (i) Three 1.5-mL centrifugal tubes were labeled as standard references 1–3 (serums containing different concentrations of inactivated hepatitis b virus), and a 400-μL lysis buffer (solution containing guanidine thiocyanate) was added to each tube. (ii) 200 μL of standard references 1–3 and 10 μL of the magnetic bead suspension (aqueous solution containing nanometer magnetic beads) were added to each tube. After shaking and mixing the mixture for 10 s, it was placed at room temperature for 10 min and then subjected to short spinning. (iii) The centrifugal tubes were placed on the magnetic frame for approximately 2 min, and the supernatant was discarded. After standing it for approximately 30 s, the residual liquid was sucked out. (iv) 600 μL of the rinse buffer (solution containing sodium chloride and ethanol) was added and pipetted 10 times and then subjected to short spinning. The centrifugal tubes were placed on the magnetic frame for approximately 2 min, the supernatant was discarded, and short spinning was performed. The tubes were then placed on the magnetic frame for approximately 2 min again, and the residual liquid was sucked out and placed at room temperature for 2 min. (v) 100 μL of the eluent buffer with high pH was added. After shaking and mixing it for 10 s, it was placed at room temperature for 2 min. The centrifugal tubes were then placed on the magnetic frame for 2 min, and the supernatant was pipetted for use. The extracted standard reference DNA templates were added to the PCR mixture as concentration gradient samples. For each experiment, 8 μL of the PCR reagent was added to the pipette connected to the aqueous-phase syringe. Driven by the syringe pump, the droplet generator produced the droplets.

2.4. Center controller and power management system

For the digital PCR device, a laptop is used as the center controller. The subsystems were connected to the laptop via serial (RS232, RS485) or USB ports. The microreactor temperature, sample transport speed, and fluorescence imaging system could be controlled by sending instructions to each subsystem from the laptop. As shown in Fig. 2, a solar cell system (12 V, 12000 mA h)

was used as the power source of the digital device. It directly supplied 12 V of power to the PID temperature controller, bus controller, and reagent refrigeration box. The 12-V power was transformed into 3-V LED power by a constant voltage module through a relay with a normally open contact.

2.5. Host computer software and data process

The host computer software is based on by Python. The graphical user interface is shown in Fig. 3. The microreactor temperature, syringe pump speed, and LED were easily controlled by the device control software. The fluorescence intensity of each droplet was obtained by fluorescence image processing using openCV. The droplets were classified as positive or negative on the basis of their fluorescence intensity. The total number of target molecules was quantified using the Poisson distribution. The probability of observing k DNA molecules in a droplet can be calculated as

$$P(X=k)=\frac{\lambda^k e^{-\lambda}}{k!} \quad (1)$$

When the initial DNA number k is 0, the droplet has negative fluorescence:

$$P(0)=e^{-\lambda}=P_{neg}$$

The numbers of negative droplets and total droplets are N_{neg} and N, respectively.

$$P_{neg}=N_{neg}/N$$

Then,

$$N_{neg}/N=e^{-\lambda}=e^{-cv}$$

The target concentration C can be estimated as

$$C=-\ln(N_{neg}/N)/V$$

where V is the volume of the PCR reagents in each droplet. The data processing can be performed automatically using the data processing software, which shows the concentration of the target in the sample, number of total droplets, number of positive droplets, number of negative droplets, and distribution and frequency of the droplet fluorescence intensity.

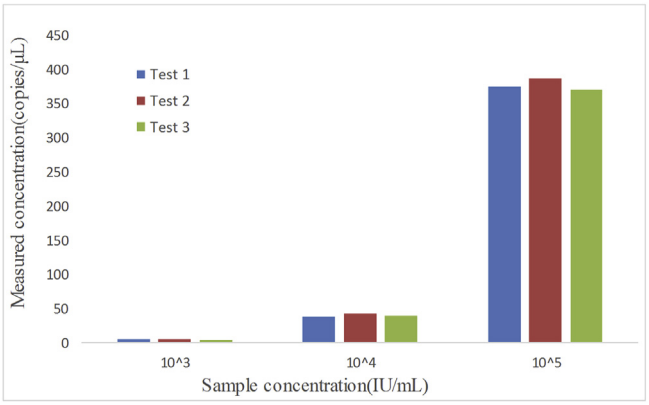

Fig. 3. Graph showing the measured concentrations of the samples.

3. Results and discussion

We evaluated the quantification of low hepatitis B virus concentrations in human serum using the proposed digital PCR device. Although the measurement of the target concentration is based on the absolute count of molecules, we additionally compared the dPCR-estimated DNA molecules with the cycle thresholds (C_t) output from the Bio-rad real-time PCR system. For the experimental testing of the dPCR device measurement capability for small amounts of DNA, qPCR measurements were performed for comparison with the dPCR results using the same measurement template.

3.1. Quantitative detection process of the digital PCR device

The digital PCR device was connected to the laptop via a USB port, and the main power switch was turned on. The PCR reagent was added to the aqueous-phase syringe and fluorinated oil was added to the oil-phase syringe. The software established serial communication with each subsystem of the device. The microreactor began to heat up, and the temperatures of the two heating plates were set to 96 °C and 62 °C, respectively. When the temperature reached the set value, the syringe pumps were started. The speed of the aqueous-phase syringe pump was set to 3 nL/s, and the speed of the oil-phase syringe pump was set to 9 nL/s. The droplets were produced

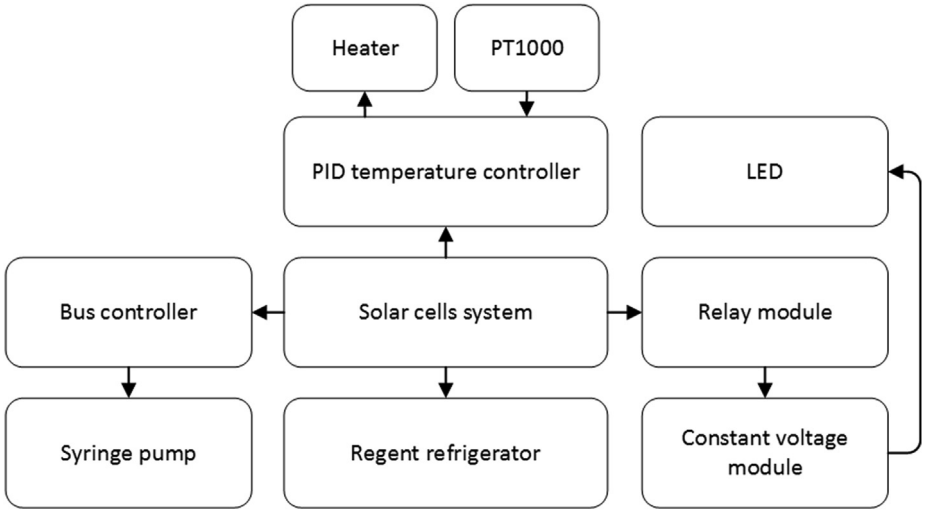

Fig. 2. Block diagram of the power electrocircuit of the continuous-flow digital PCR instrument.

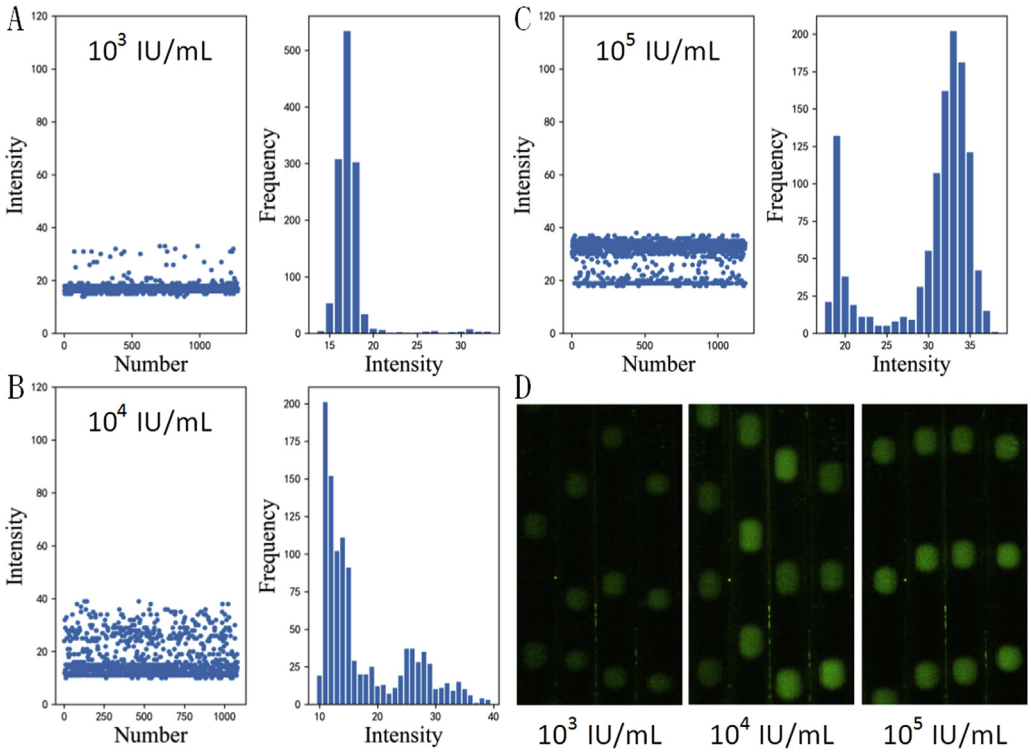

Fig. 4. (A–C) Graphs showing the distribution and frequency of the fluorescence intensity of the droplets when the concentration of the sample ranged 10^3–10^5 IU/mL. (D) The fluorescence images were captured by the CMOS camera.

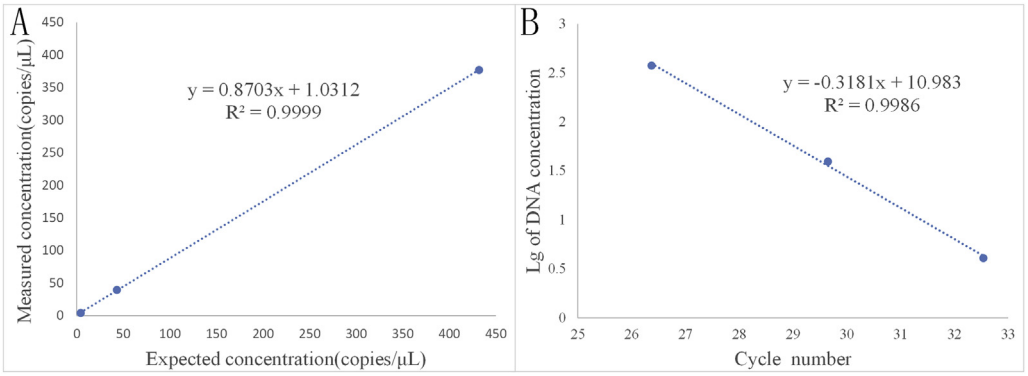

Fig. 5. (A) Correlation between the measured concentration and the expected concentration. (B) Linear correlation between the C_t values and Lg of the concentration measured using the continuous-flow digital PCR device.

by the droplet generator, and they continued to flow in the Teflon tube wrapped around the microreactor. Every time the droplets ran a cycle in the tube, the DNA was copied once. After the droplets flowed for 35 cycles, the excitation light source was activated, and the fluorescence images were captured by the CMOS camera. The captured video was analyzed by software. The number and fluorescence intensity of the droplets were measured, and the target concentration was obtained by analyzing the data. The entire instrument has a high degree of integration. It is only necessary to manually load the sample at the beginning. The final sample concentration can be obtained without manual transfer of the sample.

3.2. Results of real-time quantitative PCR and digital PCR analysis

The histogram shown in Fig. 3 presents the amplification results of the three serially ordered standard references, obtained by the continuous-flow digital PCR device. The measurement for each concentration was repeated three times. The concentrations of the standard references from 10^3 to 10^5 IU/mL were calculated as 4.39, 4.05, 3.81; 37.86, 41.28, 39.08; and 374.79, 385.93, 370.07 copies/μL, respectively. The average concentration values were 4.06, 39.40, and 376.93 copies/μL. The amplification results of the same PCR reagents obtained using the commercial qPCR cycler. The C_t values for the real-time PCR reactions were determined using a threshold detection method, and they were compared with the digital PCR results. The C_t values for the three concentrations from 10^3 to 10^5 IU/mL were 32.54, 29.65, and 26.37, respectively.

Fig. 4 shows the digital PCR detection results. The charts were automatically generated via software processing of the fluorescence image data. The fluorescence intensity distribution scatter diagrams show the fluorescence intensity of each droplet, while the frequency distribution histogram shows the number of droplets

with the same fluorescence intensity. The proportion of the low fluorescence intensity droplets decreased as the concentration of the sample increased. The negative and positive droplets could be separated by the threshold, and the concentration of the target molecule was calculated according to the Poisson distribution. The photographs show screenshots of the video captured by the CMOS camera. They depict the actual fluorescence images of the positive and negative droplets. The fluorescence intensity of the positive droplets was significantly higher than that of the negative droplets. As shown in Fig. 5 (A), a perfect linear relationship exists between the measured DNA concentrations and the theoretical concentrations of the reagents. Theoretically, the Lg of the initial concentration of the template should be linear with the cycle number. Therefore, the DNA concentrations (measured by the continuous-flow ddPCR device) and the Ct values (measured by the commercial qPCR cycler) were compared. As Fig. 5 (B) shows, the R^2 correlation coefficient between them was calculated to be 0.9986 by linear regression analysis, which proved the accuracy of the detection results of the continuous-flow ddPCR device.

4. Conclusion

This paper presented an integrated continuous-flow digital PCR system with a built-in power supply and completely designed software for equipment control and data analysis. Compared with the current commercially available digital PCR system, the proposed system has the advantages of low cost, integrated and automated operation, and portability. Further, in contrast with the existing digital PCR system, which consists of multiple independent devices, the proposed system is the first fully automatic and integrated all-in-one system. In particular, it requires only a single instance of sample loading to directly obtain the test results. Moreover, the detection results are highly reliable. The proposed device greatly simplifies the operation process without transferring samples between a series of sub-devices, and it has a wide range of application, including low-level pathogen detection, differential gene expression, absolute quantification of viral load, and copy number variation.

Declaration of competing interest

The authors declare that they have no known competing financial interests or personal relationships that could have appeared to influence the work reported in this paper.

CRediT authorship contribution statement

Yangyang Jiang: Data curation, Writing - original draft, Writing - review & editing. **Andreas Manz:** Writing - review & editing. **Wenming Wu:** Conceptualization, Funding acquisition.

Acknowledgment

This project is supported by the National Natural Science Foundation of China (No. 61704169), the CAS Pioneer Hundred Talents Program, the Natural Science Foundation of Jilin Province (20180520112JH), the Talent Project of Jilin Province, and the Fundamental Research Funds for the Central Universities.

Appendix A. Supplementary data

Supplementary data to this article can be found online at https://doi.org/10.1016/j.aca.2020.05.044.

References

[1] A. Manz, N. Graber, H.á. Widmer, Miniaturized total chemical analysis systems: a novel concept for chemical sensing, Sensor. Actuator. B Chem. 1 (1990) 244–248.
[2] P. Watts, S.J. Haswell, Microfluidic combinatorial chemistry, Curr. Opin. Chem. Biol. 7 (2003) 380–387.
[3] A. Palmieri, S.V. Ley, K. Hammond, A. Polyzos, I.R. Baxendale, A microfluidic flow chemistry platform for organic synthesis: the Hofmann rearrangement, Tetrahedron Lett. 50 (2009) 3287–3289.
[4] L.S. Roach, H. Song, R.F. Ismagilov, Controlling nonspecific protein adsorption in a plug-based microfluidic system by controlling interfacial chemistry using fluorous-phase surfactants, Anal. Chem. 77 (2005) 785–796.
[5] A.C. Sabuncu, J. Zhuang, J.F. Kolb, A. Beskok, Microfluidic impedance spectroscopy as a tool for quantitative biology and biotechnology, Biomicrofluidics 6 (2012), 034103.
[6] D.J. Ehrlich, P. Matsudaira, Microfluidic devices for DNA analysis, Trends Biotechnol. 17 (1999) 315–319.
[7] A.A. Kolodziejczyk, J.K. Kim, V. Svensson, J.C. Marioni, S.A. Teichmann, The technology and biology of single-cell RNA sequencing, Mol. Cell 58 (2015) 610–620.
[8] Y. Wang, N.E. Navin, Advances and applications of single-cell sequencing technologies, Mol. Cell 58 (2015) 598–609.
[9] L. Frenz, A. El Harrak, M. Pauly, S. Bégin-Colin, A.D. Griffiths, J.C. Baret, Droplet-based microreactors for the synthesis of magnetic iron oxide nanoparticles, Angew. Chem. Int. Ed. 47 (2008) 6817–6820.
[10] V. Taly, B.T. Kelly, A.D. Griffiths, Droplets as microreactors for high-throughput biology, Chembiochem 8 (2007) 263–272.
[11] J.H. Son, B. Cho, S. Hong, S.H. Lee, O. Hoxha, A.J. Haack, L.P. Lee, Ultrafast photonic PCR, light, Sci. Appl. 4 (2015), e280.
[12] R.A. White, P.C. Blainey, H.C. Fan, S.R. Quake, Digital PCR provides sensitive and absolute calibration for high throughput sequencing, BMC Genom. 10 (2009) 116.
[13] D. Morisset, D. Štebih, M. Milavec, K. Gruden, J. Žel, Quantitative analysis of food and feed samples with droplet digital PCR, PloS One 8 (2013), e62583.
[14] E. Mazaika, J. Homsy, Digital droplet PCR: CNV analysis and other applications, Curr. Prot. Hum. Genet. 82 (2014) 7–24.
[15] S. Dube, J. Qin, R. Ramakrishnan, Mathematical analysis of copy number variation in a DNA sample using digital PCR on a nanofluidic device, PloS One 3 (2008), e2876.
[16] R. Sanders, J.F. Huggett, C.A. Bushell, S. Cowen, D.J. Scott, C.A. Foy, Evaluation of digital PCR for absolute DNA quantification, Anal. Chem. 83 (2011) 6474–6484.
[17] B.J. Hindson, K.D. Ness, D.A. Masquelier, P. Belgrader, N.J. Heredia, A.J. Makarewicz, I.J. Bright, M.Y. Lucero, A.L. Hiddessen, T.C. Legler, High-throughput droplet digital PCR system for absolute quantitation of DNA copy number, Anal. Chem. 83 (2011) 8604–8610.
[18] C. Li, J. Xu, B. Ma, A self-powered microfluidic monodispersed droplet generator with capability of multi-sample introduction, Microfluid. Nanofluidics 18 (2015) 1067–1073.
[19] D. Bardin, A.P. Lee, Low-cost experimentation for the study of droplet microfluidics, Lab Chip 14 (2014) 3978–3986.
[20] Q. Zhu, L. Qiu, B. Yu, Y. Xu, Y. Gao, T. Pan, Q. Tian, Q. Song, W. Jin, Q. Jin, Y. Mu, Digital PCR on an integrated self-priming compartmentalization chip, Lab Chip 14 (2014) 1176–1185.
[21] Y. Wang, K.M. Southard, Y. Zeng, Digital PCR using micropatterned superporous absorbent array chips, Analyst 141 (2016) 3821–3831.
[22] J.-L. He, A.-T. Chen, J.-H. Lee, S.-K. Fan, Digital microfluidics for manipulation and analysis of a single cell, Int. J. Mol. Sci. 16 (2015) 22319–22332.
[23] D.-K. Kang, M.M. Ali, K. Zhang, S.S. Huang, E. Peterson, M.A. Digman, E. Gratton, W. Zhao, Rapid detection of single bacteria in unprocessed blood using Integrated Comprehensive Droplet Digital Detection, Nat. Commun. 5 (2014) 5427.
[24] R. Sista, Z. Hua, P. Thwar, A. Sudarsan, V. Srinivasan, A. Eckhardt, M. Pollack, V. Pamula, Development of a digital microfluidic platform for point of care testing, Lab Chip 8 (2008) 2091–2104.
[25] A.C. Hatch, J.S. Fisher, A.R. Tovar, A.T. Hsieh, R. Lin, S.L. Pentoney, D.L. Yang, A.P. Lee, 1-Million droplet array with wide-field fluorescence imaging for digital PCR, Lab Chip 11 (2011) 3838–3845.
[26] S.H. Kim, S. Iwai, S. Araki, S. Sakakihara, R. Iino, H. Noji, Large-scale femtoliter droplet array for digital counting of single biomolecules, Lab Chip 12 (2012) 4986–4991.
[27] A.E. Cetin, A.F. Coskun, B.C. Galarreta, M. Huang, D. Herman, A. Ozcan, H. Altug, Handheld high-throughput plasmonic biosensor using computational on-chip imaging, Light: Sci. Appl. 3 (2014) e122.
[28] H. Ren, R.B. Fair, M.G. Pollack, Automated on-chip droplet dispensing with volume control by electro-wetting actuation and capacitance metering, Sensor. Actuator. B Chem. 98 (2004) 319–327.
[29] J. Floury, A. Desrumaux, J. Lardières, Effect of high-pressure homogenization on droplet size distributions and rheological properties of model oil-in-water emulsions, Innovat. Food Sci. Emerg. Technol. 1 (2000) 127–134.
[30] W. Stephenson, L.T. Donlin, A. Butler, C. Rozo, B. Bracken, A. Rashidfarrokhi, S.M. Goodman, L.B. Ivashkiv, V.P. Bykerk, D.E. Orange, Single-cell RNA-seq of rheumatoid arthritis synovial tissue using low-cost microfluidic

instrumentation, Nat. Commun. 9 (2018) 791.
[31] E. Samiei, M. Tabrizian, M. Hoorfar, A review of digital microfluidics as portable platforms for lab-on a-chip applications, Lab Chip 16 (2016) 2376–2396.
[32] H. Tanaka, S. Yamamoto, A. Nakamura, Y. Nakashoji, N. Okura, N. Nakamoto, K. Tsukagoshi, M. Hashimoto, Hands-off preparation of monodisperse emulsion droplets using a poly (dimethylsiloxane) microfluidic chip for droplet digital PCR, Anal. Chem. 87 (2015) 4134–4143.
[33] Y. Fu, H. Zhou, C. Jia, F. Jing, Q. Jin, J. Zhao, G. Li, A microfluidic chip based on surfactant-doped polydimethylsiloxane (PDMS) in a sandwich configuration for low-cost and robust digital PCR, Sensor. Actuator. B Chem. 245 (2017) 414–422.